PEER-REVIEWED ARTICLE

Discrimination of Subalpine Forest Species and Canopy Density Using Digital CASI, SPOT PLA, and Landsat TM Data

Steven E. Franklin

Abstract

The number of forest attributes which can be remotely sensed with sufficient precision and accuracy for stand inventory purposes is large, and as yet not fully identified, for different sensor systems and under a variety of forest conditions. In this paper, three digital image data sets were compared and used to discriminate a range of forest cover types in the Subalpine Forest Region west of Calgary, Alberta, Canada. Compact Airborne Spectrographic Imager (CASI) data, SPOT Panchromatic Linear Array (PLA) data, and Landsat Thematic Mapper (TM) data were collected over forest stands that differed in species, density, and height. As in previous studies of mountainous areas, a digital elevation model (DEM) was used to increase classification accuracy (measured as the percent agreement with conventional aerial photointerpretation and field observations) to more acceptable levels. For example, the PLA data did not contain enough information to discriminate the training sample with better than about 50 percent of the sites correctly classified; but accuracies up to 74 percent were achieved when DEM data were added to the decision rules for this same sample. Various combinations of the TM and CASI image data both alone and augmented with elevation and first-order derivatives were tested, with best accuracies above 90 percent. Correlation matrices were also constructed and interpreted for these data to study the effect of differing spectral and spatial resolutions, and the topographic effect on discrimination of forest inventory parameters.

Introduction

In different regional settings (Williams and Nelson, 1986; Fleming, 1988; Hopkins *et al.*, 1988; Borry *et al.*, 1990), spectral response in visible and infrared wavelengths measured by satellite and aerial sensors has been shown to vary significantly with forest attributes such as species, crown or canopy density, height, volume, health, and age (Horler and Ahern, 1986; Franklin, 1986; Vogelmann and Rock, 1986; Danson, 1987; Dewulf *et al.*, 1990; Peterson *et al.*, 1988; Plummer, 1988, Running *et al.*, 1989; Khorram *et al.*, 1990; Cohen *et al.*, 1990; Ahern *et al.*, 1991; Brockhaus *et al.*, 1992; Brockhaus and Khorram, 1992). In mountainous areas, image variance can be influenced by the topographic effect (Holben and Justice, 1981; Hall-Konyves, 1987; Leprieur *et al.*, 1988; Franklin, 1992) and the reflectance anisotropy of vegetated surfaces (Irons *et al.*, 1987; 1991; Kriebel, 1978). Atmospheric constituents, size of the viewed area, and the geometrical and optical properties of the surface cover, underlying soil, and background may also contribute additional variance (Guyot *et al.*, 1989). Discriminating forest inventory characteristics from this background "noise" has been discussed for a variety of sensors ranging from aerial video instruments (Vlcek and King, 1985; Yuan *et al.*, 1991) to coarse resolution spaceborne scanners (Walsh, 1987; Ripple *et al.*, 1991). However, for a variety of reasons perhaps related to scale and cost, human interpretation of aerial photographs (Avery and Berlin, 1992) continues to be the remote sensing methodology of choice in forest inventory.

New sensors have been developed to provide general purpose multispectral imaging with specific applications in forestry and ecology (Irons *et al.*, 1991; Staenz, 1992) and agriculture (Hutchinson *et al.*, 1990). In at least one case—the Multi-detector Electro-optical Imaging Sensor for Forestry and Mapping (MEIS-FM) developed by the Canada Centre for Remote Sensing (CCRS)—the sensor is intended to replace aerial photography in forestry and mapping studies (Neville and Till, 1991; Hegyi *et al.*, 1992).

Another instrument—the Compact Airborne Spectrographic Imager (CASI)—is a new Canadian pushbroom sensor designed specifically to enable low-cost acquisition of multispectral imagery (Babey and Anger, 1989; Gower *et al.*, 1992) for aquatic and terrestrial studies. The instrument is based on a two-dimensional frame transfer CCD array. The sensing head employs a fast (*f*/2) reflection grating spectrograph with a wavelength range of 400 to 900 nm and a sampling interval of 1.8 nm. A distinguishing feature of the system is the fully programmable spectral bandsets during image acquisition from light aircraft in either (1) spectral mode (maximum 288 bands) or (2) spatial mode (maximum 15 bands) with a 12-bit dynamic range. The data are recorded on low cost 8-mm video cassettes in a format suitable for direct input to digital image analysis systems. A Global Positioning System/Inertial Navigation System (GPS/INS) capability has been developed to georeference CASI data during image acquisition (Ivanco *et al.*, 1991; Cosandier *et al.*, 1992).

Encouraging results have been obtained with the CASI and earlier prototypes in surface fish school surveys (Nakashima *et al.*, 1989; Borstad *et al.*, 1992), mapping phytoplankton (Gower and Borstad, 1990) and ocean vegetation (Zacharias *et al.*, 1992), derivation of vegetation red edge

Department of Geography, The University of Calgary, Calgary, Alberta T2N 1N4, Canada.

Photogrammetric Engineering & Remote Sensing, Vol. 60, No. 10, October 1994, pp. 1233–1241.

0099-1112/94/6010-1233$3.00/0

parameters (Miller *et al.*, 1991), and spectral signature analysis of vegetation (Gong *et al.*, 1992) and artificial surfaces such as asphalt (Royer *et al.*, 1989). The discriminating capabilities of this sensor have not been explored fully or compared to other data sources in operational forestry remote sensing applications, such as forest stand structure mapping, which is a critical step in forest inventory. Therefore, this paper provides an initial assessment of CASI data for classifying forests using relatively straightforward classification techniques and with the integration of a digital elevation model (DEM).

In an earlier study (Franklin *et al.*, 1991), the angular reflectance patterns of forest canopies captured in CASI data were examined for a mountainous region in southwestern Alberta, Canada. The separation of three deciduous species and one coniferous species in pure stands was reported, but the sample was small, limiting our confidence in the result. In this paper, the discrimination is conducted on a larger sample and in mixed stands having different density and height characteristics. The high resolution CASI data are compared to near-coincident SPOT Panchromatic Linear Array (PLA) imagery, and to an historical Landsat Thematic Mapper (TM) image.

Objectives

The objectives of this study were to investigate the topographic effect on spectral response at different spectral and spatial resolutions, and to determine the classification accuracy for different forest stands that can be achieved with various combinations of remotely sensed (CASI, PLA, TM) and geomorphometric discriminators. It is a central hypothesis of our continuing work in remote sensing of Canadian forests that stands considered distinct for inventory purposes using conventional aerial photointerpretation techniques can be separated consistently using digital data and classification methods. Results are discussed with reference to additional improvements that may be possible through image texture processing (Peddle and Franklin, 1991), multisource evidential reasoning (Peddle and Franklin, 1992), and multistage classifiers which employ spatial image attributes (Franklin and Wilson, 1992).

Study Area

The area of study is located in the Bow Crow Provincial Forest in southern Alberta on the eastern slope of the Canadian Rocky Mountains (Figure 1). The site is typical of the Canadian Subalpine Forest Region, was heavily glaciated in the Pleistocene, and contains relationships between site conditions, soil texture, and forest productivity similar to those described by Kirby (1973) in an area 20 km to the south of the present study site. The dominant forest species are lodgepole pine (*Pinus contorta*) with mixed stands of Engelmann spruce (*Picea engelmannii*) and white spruce (*Picea glauca*). Deciduous species found in pure stands are aspen (*Populus tremuloides*) and balsam poplar (*Populus balsamifera*) with small isolated stands of cottonwood (*Populus trichocarpa*). The floodplains of the small mountain streams are terraced and support grassland communities. Wetlands are diverse but not extensive. Forest stand distribution and condition may be explained largely by drainage, topography, fire history, and recent cultural developments.

Active forestry practices in this region include clearcutting, selective cutting, plantation establishment, silvicultural pruning and thinning, fire suppression, and insect population control. The most recent forest inventory for this region

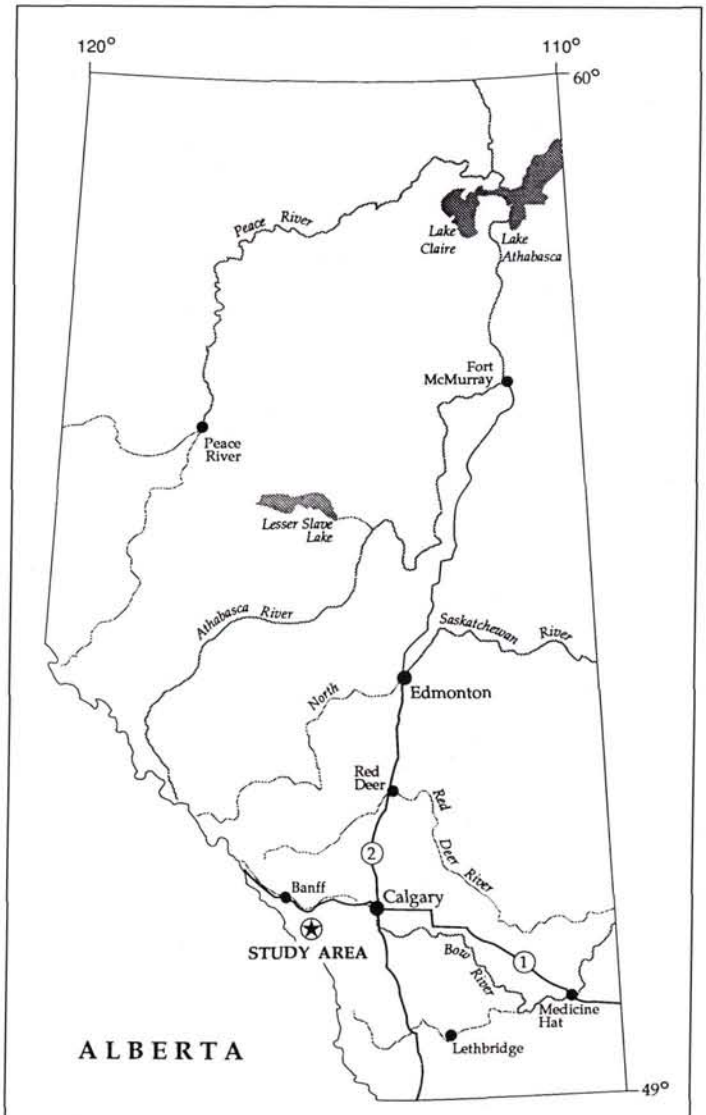

Figure 1. Location of the study area in southwestern Alberta.

was compiled using conventional aerial photointerpretation based on 1:20,000-scale color aerial photographs acquired in 1982 and 1:20,000-scale black-and-white photographs acquired in 1987. Operational cruising was conducted in 1988, resulting in new inventory maps published in 1989, which included stand information on species composition, stand density, dominant tree height and age classes, and stand boundaries.

Data Collection and Methodology

The CASI data were collected on 8 August 1990 in spatial mode at 2.5-metres ground cell resolution through a clear atmosphere. Nine spectral channels (Table 1) were recorded on two flight lines flown east to west then west to east at approximately 13:15 MDT, with an average solar zenith angle of 54° and sun azimuth of 167°. These CASI data were acquired in support of a study of surface reflectance anisotropy over dense pine canopies (Franklin *et al.*, 1991).

TABLE 1. CASI BANDSET

Band 1	491 – 499nm
Band 2	547 – 556nm
Band 3	597 – 606nm
Band 4	638 – 646nm
Band 5	671 – 682nm
Band 6	702 – 709nm
Band 7	745 – 749nm
Band 8	754 – 756nm
Band 9	788 – 808nm

The Landsat Thematic Mapper data were acquired 8 August 1985; the SPOT PLA panchromatic data were acquired 6 August 1990. No atmospheric corrections were applied, but the imagery were without visible radiometric or atmospheric degradation when viewed on the image analysis color display. The wide variation in image dates could be expected to have an impact on the results of this study, particularly as they relate to stand structure properties.

Three subareas measuring approximately 25 square kilometres each were extracted from the flight lines and satellite imagery that included varying topographic conditions and forest stands with different species, height, and density characteristics. The inventory information was obtained from the 1989 inventory maps and verified with the 1:20,000-scale color aerial photography and two field visits in November 1990 and August 1991. Vector point files of the selected subareas were digitized from 1:50,000-scale topographic map sheets. A dense grid of elevation data points was interpolated using the Surface II Graphics System (Davis, 1987) with a distance-weighted average of the nearest 16 points. Computer programs were written to convert the output digital elevation model binary files into a format compatible with the available image analysis system (PCI Inc., 1992). The DEMs were registered and "rubber-sheeted" to the CASI data with a 1.5-pixel error tolerated in the resampling. Similarly, the DEMs were registered and resampled to fit the TM image and the SPOT PLA image. No resampling of the aerial or satellite imagery was done.

Geomorphometric Processing

The DEMs were smoothed and processed for variables which conform to the general system of geomorphometry. Evans (1972) defined this system of terrain descriptors based on derivatives and moments of the distributions of a few fundamental measurements or properties that apply to a continuous, varying surface. Slope angle (first vertical derivative of elevation) and aspect angle (first horizontal derivative of elevation) for each pixel were calculated using the partial derivatives of the elevation values with respect to the X (east/west) and Y (north/south) directions. The partial derivatives can be determined using two 3 by 3 first-order filters (Sobel operators). The slope and aspect were then calculated as follows:

$$\text{slope} = \tan^{-1}\{[(\partial z/\partial x)^2 + (\partial z/\partial y)^2]^{1/2}\} \quad (1)$$

$$\text{aspect} = \tan^{-1}[(-\partial z/\partial y)/(-\partial z/\partial x)]. \quad (2)$$

The calculation essentially fits a second-order surface to the neighborhood based on a minimum mean-squared error criterion (Franklin, 1987). The derivatives were smoothed twice using a 5 by 5 spatial filter to eliminate linear (contour line) artifacts.

Incidence value was defined as the normalized cosine of slope and aspect relative to the solar position during image acquisition:

$$\text{Incidence} = \cos(\alpha) + \sin(\alpha) * \cot(\beta) * \cos(\theta) \quad (3)$$

where α is slope, β is sun elevation, and θ is the difference between terrain aspect on a compass and the solar azimuth. Each term is expressed in degrees. The incidence value represents an estimate of the ratio of direct solar illumination and a diffuse component. Terrain aspects in total shadow receive only diffuse radition, and may have a negative incidence value. No consideration of backscatter, adjacent slope flux, or horizon brightening is given. In the general linear models described below, incidence values are used in place of aspect (which is a circular variable and must be interpreted separately).

Image Training and Sampling

Correlation statistics and scatterplots were generated from random samples to show the relationships between spectral variables and geomorphometric variables.

Discriminant analysis requires that samples be drawn from known classes in a straightforward supervised procedure. During training pixel collection, an effort was made to derive pixel values from the same stands from each separate image data set. The pixel-by-pixel training method suggested by Gong and Howarth (1990) was employed with the resulting attribute tables subjected to statistical modeling using SPSSx (SPSSx Inc, 1986). Discriminant functions were generated for each of the inventory classes listed in Table 2 for each of the three areas. Because no independent test areas were available in support of this analysis, training data were

TABLE 2. FOREST INVENTORY CLASSES

Class	Description	Density (%)	Height (m)	Label	Color in Plate 1
1	Cultural	—	— —	Cul	Orange
2	Grassland	—	— —	Grs	Green
3	Aspen & Balsam Poplar	51–70	12.1–18.0	C2AB	Magenta
4	White Spruce & Balsam Poplar	51–70	12.1–18.0	C2SwB	Brown
5	Aspen & White Spruce	51–70	12.1–18.0	C2ASw	Purple
6	White Spruce & Aspen	51–70	18.1–24.0	C3SwA	Pink
7	Pine & White Spruce	51–70	18.1–24.0	C3PSw	Gray
8	Pine & White Spruce	71–100	12.1–18.0	D2PSw	Red
9	Pine	71–100	6.1–12.0	DIP	Cyan
10	Pine	6–30	6.1–12.0	A1P	Blue
11	Pine, White Spruce & Aspen	71–100	12.1–18.0	D2PSwA	Black

TABLE 3. BIVARIATE CORRELATIONS AMONG SPECTRAL AND DEM VARIABLES, N = 4590

	S1	C1	C2	C3	C4	C5	C6	C7	C8	C9	E	SL	IN	T1	T2	T3	T4	T5
C1	0.83																	
C2	0.84	0.94																
C3	0.86	0.98	0.98															
C4	0.84	0.99	0.95	0.99														
C5	0.85	0.99	0.93	0.98	0.99													
C6	0.78	0.85	0.96	0.90	0.87	0.83												
C7	0.21	0.16	0.37	0.22	0.15	0.12	0.54											
C8	0.18	0.11	0.31	0.16	0.10	*	0.47	0.99										
C9	0.18	0.11	0.32	0.17	0.11	*	0.48	0.99	0.99									
E	*	−0.19	−0.18	−0.13	−0.13	−0.13	−0.17	−0.33	−0.35	−0.35								
SL	−0.19	−0.25	−0.25	−0.23	−0.22	−0.22	−0.25	−0.21	−0.20	−0.18	0.49							
IN	0.36	0.18	0.27	0.23	0.21	0.19	0.31	0.29	0.30	0.29	*	−0.33						
T1	0.92	0.72	0.77	0.78	0.75	0.74	0.73	0.16	0.13	0.14	*	*	0.37					
T2	0.91	0.72	0.78	0.79	0.75	0.75	0.75	0.20	0.16	0.17	0.12	*	0.43	0.98				
T3	0.90	0.73	0.79	0.80	0.76	0.75	0.75	0.14	*	0.10	0.14	*	0.39	0.98	0.98			
T4	0.11	*	*	*	*	*	*	0.67	0.73	0.72	−0.22	*	0.33	*	*	*		
T5	0.77	0.55	0.68	0.64	0.58	0.56	0.70	0.44	0.42	0.43	0.20	*	0.55	0.84	0.88	0.84	0.39	
T7	0.85	0.67	0.75	0.74	0.70	0.68	0.73	0.22	0.18	0.19	0.25	*	0.45	0.94	0.95	0.95	*	0.93

(* Denotes Correlation Not Significant at P=0.01)
(** Variables S1=SPOT Panchromatic; C1=CASI Bandset; E, SL, IN=elevation, slope, incidence; T1–T5,T7=TM Bandset)

divided randomly into two equal sets of pixels per class for training and testing the funcitons. The results are reported for all three areas combined (n=4590) and for one of the small subareas (n=1530) containing representative samples. Classification accuracy in this study was the average of the diagonal entries in contingency tables produced for each function. Classification maps for the small subarea summarized in Table 5 are shown in Plate 1 to illustrate the spatial arrangement of forest stands.

Results and Discussion

Table 3 lists the bivariate correlations between all spectral bands used in the study and the three geomorphometric parameters derived from the elevation model. Each TM band is significantly related to incidence, but none of these data are related to slope ($p<0.01$). The SPOT data are also positively correlated with incidence, and are negatively (but weakly) related to slope. The CASI data illustrate this same pattern, but also show higher correlation to elevation. Within the geomorphometric parameters, slope and incidence are negatively correlated, slope and elevation are positively correlated, and incidence and elevation are not correlated ($p<0.01$). As slopes increase, elevation increases, and incidence values tend to decrease, which is interpreted to mean that steep slopes tend to face away from the Sun in this area.

Spectral dependence on incidence values is one way to quantify the topographic effect (Woodcock, 1982; Leprieur *et al.*, 1988), and to illustrate the importance of considering topographic variations in spectral response. The TM dependence on incidence is greater than the dependence in the other two data sets; this may be a function of the coarser resolution of the TM image which contains less variance over small areas. Within the CASI and TM data sets, higher correlation coeficients are observed in the infrared parts of the spectrum. In the earlier study (Franklin *et al.*, 1991) this effect was attributed to the increased atmospheric scattering at shorter wavelengths (which were not removed in these data), or to increased reflectance anisotropy in the infrared bands.

One interpretation of these correlation results is related to the predicted performance of the spectral and geomorphometric variables in classification algorithms. First, because the target classes of interest (forest species and density classes) are related to topography in this area (Kirby, 1973), there exists an *a priori* rationale to include geomorphometry as discriminating variables in a classification. Second, some spectral variance is dependent on geomorphometry, or is topographically induced. The explicit inclusion of topography in the form of slope, aspect, and elevation may produce increases in classification accuracy where such information is independent and unique.

Table 4 contains a summary of the classification results derived using the various discriminant funcitons with and without the addition of digital elevation model variables. The overall classification accuracy using the CASI data alone was 81 percent. This increased to 90 percent using the full set of CASI and DEM data. Essentially the same figures were obtained in classifying the TM image using the TM alone and TM plus DEM functions. The SPOT imagery performed much less well, with a PLA alone result of 49 percent and a PLA plus DEM result of 74 percent. The DEM was used to classify the inventory stands with 48 percent accuracy overall; but it is interesting to note that pure coniferous stands were classified accurately 80 percent of the time on the basis of topographic variables alone. The individual class accuracies are reported in Table 5, and Plate 1 shows the distribution of the classes for the TM and CASI classifications.

The CASI and TM results were remarkably similar throughout the discrimination. Some differences were revealed in the discrimination of pure stands of different density (CASI 93 percent, TM 96 percent), mixed coniferous species of different heights (CASI 67 percent, TM 84 percent), mixed deciduous stands (CASI 73 percent, TM 80 percent), and mixed deciduous and coniferous stands (CASI 78 percent, TM 82 percent). In all these cases, the TM data performed marginally better than the CASI, and much better than the single band SPOT data. As predicted in the earlier correlation analysis, the topographic effect was most pronounced in the TM image and translated into a relatively larger increase in accuracy than for the CASI data. The overall increases in accuracy after addition of the DEM variables was approximately 8 percent for the CASI image and 11 percent for the TM image. The corresponding SPOT discrimination in-

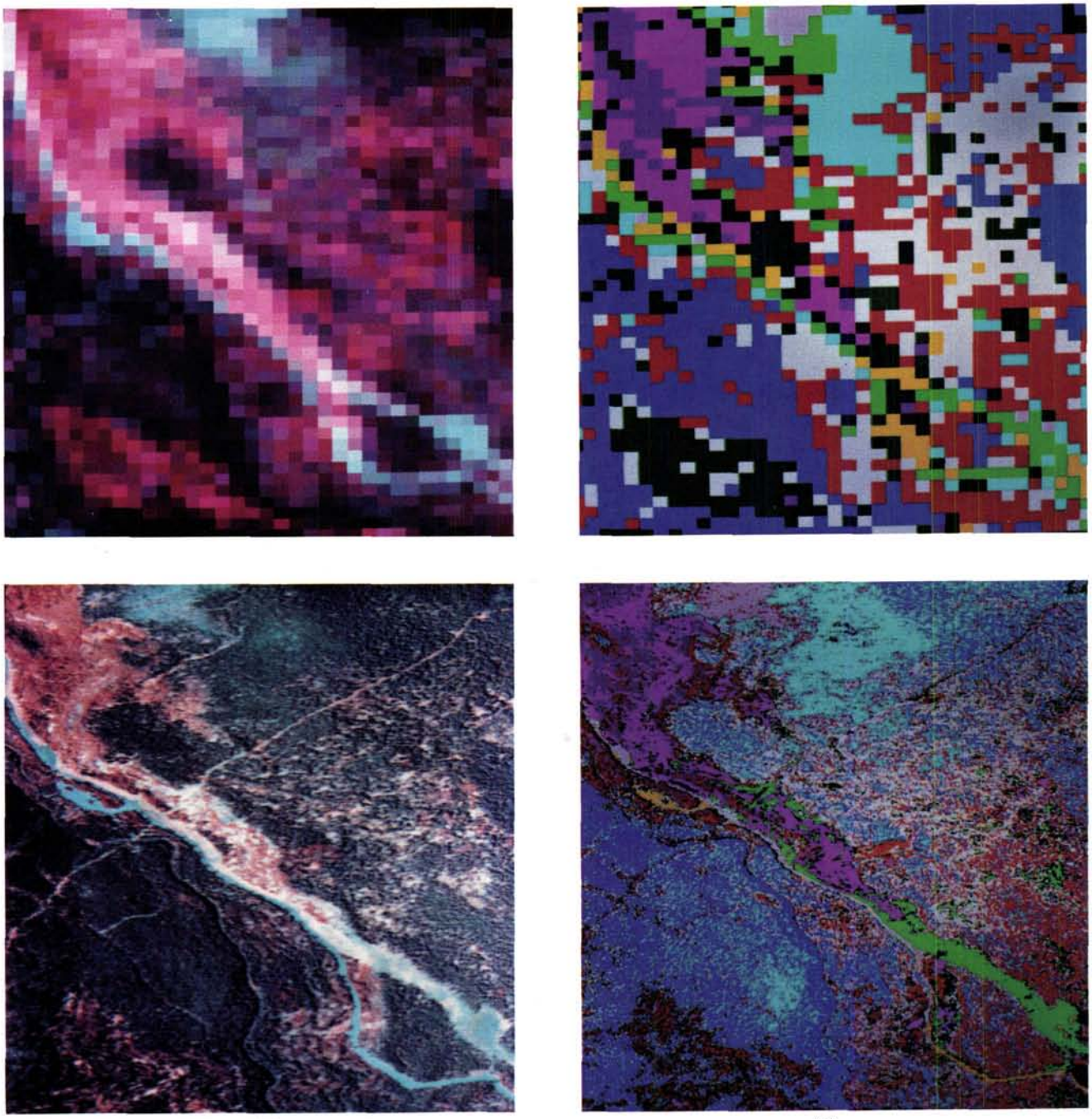

(c) (d)

Plate 1. TM and CASI image composites with corresponding classification maps (colors/classes in Table 2) (approx. area 1.5 km by 1.5 km). (a) TM bands 2,4,7: 30-m resolution: representing L-resolution image. (b) Classified TM image: accuracy approximately 81 percent tested at more than 1500 sites. (c) CASI bands 2,4,7: 2.5-m resolution: representing H-resolution image. (d) Classified CASI image: accuracy approximately 82 percent tested at more than 1500 sites.

creased more than 24 percent, but this is a reflection of the overall poor ability of the SPOT data to separate the stands, rather than a function of topographically induced variance in the imagery. The largest increases in accuracy were noted in mixed stands for the CASI and the TM imagery, and in pure coniferous stands for the SPOT image.

The good agreement between CASI, TM, and forest inventory maps derived from aerial photographs is attributed to

TABLE 4. OVERALL CLASSIFICATION ACCURACY FOR SELECTED DISCRIMINANT FUNCTIONS, N = 4590

Function	Mean Class Accuracy
DEM Alone	48.59%
SPOT Panchromatic Alone	49.23%
SPOT Panchromatic & DEM	74.36%
TM Alone	81.03%
TM & DEM	91.31%
CASI Alone	81.39%
CASI & DEM	89.66%

the high spectral resolution available in these data, and in a seeming contradiction, both to the very high (CASI) and relatively coarse (TM) spatial resolution. Adopting the terminology of Stahler *et al.* (1986) and Jupp *et al.* (1988; 1989), the CASI data are a High-resolution source (H), and the TM data are a Low-resolution source (L). In the CASI data, the pixels in the image are much smaller than the objects in the scene; i.e., individual trees are resolved. The local variance is low because many adjacent pixels take on similar values, either the object or the background. But, true variability of the stand has not been characterized because anomalous pixels are avoided (e.g., shadows, background pixels) during the collection of training pixels (see for example, Hughes *et al.* (1986)). In the TM image, training is done in the same stands, but the pixel size is sufficiently large to subsume many individual trees and other features; the pixels are much larger than the objects in the scene. If the density of the objects is more or less uniform, then adjacent pixels in the stand will have more or less similar values. The local variance will again be low. This composite pixel has been shown to be distinct from composite pixels acquired in different inventory stands in the discrimination.

Some interesting questions may now be posed relating to the textural quality of the data in these two cases (Plate 1). Clearly, the CASI data are "inherently" more textural, and their analysis would receive relatively greater benefit after texture processing. It is probable that, if the purpose of the discrimination is to produce classification maps with standard supervised classification methods (such as those in Plate 1), the CASI would perform much less well than in the per-pixel discrimination (such as in Table 5). Higher local variance would be required in the training of such a classifier which would translate into poorly parameterized classes (i.e., the means and variances would not represent the trees only, but the trees plus the background, ensuring large class overlap). Therefore, while the CASI data *discriminate* well the required inventory stands, this does not necessarily mean that the stands can be *mapped* well. Similarly, the TM data illustrate the problems with an L-resolution source if the objective is to produce maps of the forest stands. In this case, the stands which violate the assumption of uniform object density (such as in mixed or young stands), are mapped by TM data as a mixture of classes rather than as a single class. Some additional post-classification processing (Thomas, 1980; Booth *et al.*, 1989; Franklin and Wilson, 1992) may alleviate some of these mapping problems. Non-parametric classifiers (Skidmore and Turner, 1988), or new formulations of decision rules (Spann and Wilson, 1985; Bolstad and Lillesand, 1992) may be needed which are less sensitive to class statistics such as mean spectral response and covariance.

The SPOT image similarly generates a composite pixel; however, poor discrimination shows that the lack of spectral dimensions reduces the information content to low levels. Although the pixel size in this image is larger than the object size, the appropriate place for the SPOT 10-m pixel in the H-resolution or L-resolution models has not been defined.

Conclusions

The number of forest inventory parameters that can be remotely sensed and extracted from digital imagery is large, and as yet not fully identified, for a variety of sensors and a range of forest cover types. In this study, three digital images from a new aerial sensor (CASI) and the SPOT PLA and Landsat TM sensors were compared and used to discriminate mixed and pure forest stand types of varying density and height in the subalpine region of Alberta, Canada. A digital elevation model was generated and integrated with the imagery to study topographic effects, and the relative increases in accuracy in classifications that consider geomorphometric and spectral variance. The topographic effect (estimated as the correlation between spectral response and incidence values) was most pronounced in the TM image. The general increase in accuracy for the aerial CASI data combined in a discriminant function with DEM data was approximately 8 percent, with the best classification accuracy achieved equal to 90 percent agreement with the forest inventory. Corresponding figures of 11 percent increase and 91 percent overall accuracy were obtained for the TM image.

TABLE 5. CLASSIFICATION ACCURACY BY CLASS FOR SELECTED FUNCTIONS IN ONE SUB AREA, N = 1590

Function	Percent Classified into Class*											
	1	2	3	4	5	6	7	8	9	10	11	X
CASI	100	93	73	60	100	67	87	47	93	93	67	80.9
DEM	73	47	60	0	33	43	57	33	67	93	0	45.7
CASI & DEM	100	93	87	73	97	77	93	73	87	100	87	88.1
SPOT PAN	80	47	93	—	67	7	73	20	20	73	33	51.3
DEM	40	0	7	—	73	73	100	13	87	87	27	50.7
SPOT PAN & DEM	93	60	80	—	73	73	100	40	100	100	47	76.7
TM	87	87	80	—	93	87	80	80	100	93	67	85.3
DEM	53	0	67	—	80	60	87	47	60	87	0	54.0
TM & DEM	80	93	80	—	93	100	100	87	93	100	93	92.0

(* Classes: 1 = Cultural, 2 = Grassland, 3 = Aspen & Balsam Poplar, 4 = White Spruce & Balsam Poplar, 5 = Aspen & White Spruce, 6 = White Spruce & Aspen, 7 = Pine & White Spruce, 8 = Pine & White Spruce, 9 = Pine, 10 = Pine, 11 = Pine, White Spruce & Aspen; See Table 2 for details on density height and species composition).

SPOT PLA data were used with the DEM to obtain 74 percent accuracy, which was a 24 percent increase over the accuracy obtained with the SPOT image alone. These data did not contain spectral details sufficient to produce accurate classifications by discriminant functions. Geomorphometric variables alone yielded 48 percent agreement with the forest inventory.

The CASI and TM discriminant results were remarkably similar but for different reasons. The CASI produced good agreement with the forest inventory because of very high spatial resolution, with individual tree and forest parameters resolved, while the TM image produced similar levels of accuracy because of coarse spatial resolution. Based on this successful discrimination of species and canopy density, operational problems in using such H-resolution (CASI) or L-resolution data (TM) sources for *mapping* purposes were identified and must be addressed.

This study complements an earlier analysis of the surface reflectance anisotropy captured in CASI data and the discrimination of deciduous species in pure stands (Franklin *et al.*, 1991), and confirms both (1) the utility of CASI data in forestry applications and (2) the relative importance of digital elevation models for separation and analysis of Canadian forest inventory parameters in this rugged mountain environment. Further work is planned on the textural aspects of these data (Peddle and Franklin, 1991), the use of evidential reasoning models to overcome limitations in statistical classifiers (Peddle and Franklin, 1992), and the development of customized spatial classifiers (Frank and Wilson, 1992) which can employ different image signatures to classify the parts (in this case, inventory stands) of the imagery for which they are best suited.

Acknowledgments

Financial support was provided by the Natural Sciences and Engineering Research Council and the University of Calgary. Aerial data acquisition was arranged by Cathy Wrightson (ITRES Research Ltd.). Steven Mah and Clayton Blodgett prepared the data base and Ron Peart performed some of the image analysis while supported by an Alberta STEP grant.

References

Ahern, F. J., T. Erdle, D. A., MacLean, and I.D. Kneppeck, 1991. A quantitative relationship between forest growth rates and Thematic Mapper reflectance measurements, *International Journal of Remote Sensing*, 12(3): 387–400.

Avery, T. E., and G. Berlin, 1992. *Fundamentals of Remote Sensing and Airphoto Interpretation*, Fifth Edition, MacMillan, New York, 472 p.

Babey, S. K., and C. D. Anger, 1989. A Compact Airborne Spectrographic Imager (CASI), *Proceedings, International Geoscience and Remote Sensing Symposium*, Vancouver, Canada, pp. 1028–1031.

Bolstad, P., and T. Lillesand, 1992. Rule-based classification models: flexible integration of satellite imagery and thematic spatial data, *Photogrammetric Engineering & Remote Sensing*, 58(7): 965–971.

Booth, D. J., T. Chidley, and W. G. Collins, 1989. Integration of context classifiers with GIS, *Proceedings, International Geoscience and Remote Sensing Symposium*, Vancouver, Canada, pp. 656–659.

Borry, F. C., B. P. DeRoover, R. R. DeWulf, and R. E. Goossens, 1990. Assessing the value of monotemporal SPOT-1 imagery for forestry applications under Flemish conditions, *Photogrammetric Engineering & Remote Sensing*, 56(8): 1147–1154.

Borstad, G. A., D. A. Hill, R. C. Kerr, and B. S. Nakashima, 1992. Direct digital remote sensing of herring schools, *International Journal of Remote Sensing*, in press.

Brockhaus, J. A. and S. Khorram. 1992. A comparison of SPOT and Landsat TM data for use in conducting inventories of forest resources. *International Journal of Remote Sensing*, 13(16): 3035–3043.

Brockhaus, J. A., S. Khorram, R. I. Bruck, M. V. Campbell, and C. Stallings, 1992. A comparison of Landsat TM and SPOT HRV data for use in the development of forest defoliation models, *International Journal of Remote Sensing*, 13(16): 3235–3240.

Cohen, W., T. A. Spies, and G. A. Bradshaw, 1990. Semivariograms of digital imagery for analysis of conifer canopy structure, *Remote Sensing of Environment*, 34: 167–178.

Cosandier, D., T. Ivanco, and S. Mah, 1992. The geocorrection and integration of the global positioning system with the Compact Airborne Spectrographic Imager, *Proceedings, 15th Canadian Symposium on Remote Sensing*, Toronto, Ontario, pp. 385–390.

Danson, F. M., 1987. Preliminary evaluation of the relationships between SPOT-1 HRV data and forest stand parameters, *International Journal of Remote Sensing*. 8(10): 1571–1575.

Davis, J. 1987. Contour mapping and Surface II, *Science*, 237: 669–672.

DeWulf, R. R., R. E. Goossens, B. P. De Roover, and F. C. Borry, 1990. Extraction of forest stand parameters from panchromatic and multispectral SPOT-1 data, *International Journal of Remote Sensing*, 11(9): 1571–1588.

Evans, I.S., 1972. General geomorphometry, derivatives of altitude and descriptive statistics, *Spatial Analysis in Geomorphology*, (R.J. Chorley, editor), Methuen, London, pp. 17–90.

Fleming, M., 1988. An integrated approach for automated cover-type mapping of large inaccessible areas in Alaska, *Photogrammetric Engineering & Remote Sensing*, 54(3): 357–362.

Franklin, J., 1986. Thematic Mapper analysis of coniferous forest structure and composition, *International Journal of Remote Sensing*, 7(10): 1287–1301.

Franklin, S. E., 1987. Geomorphometric processing of digital elevation models, *Computers and Geosciences*, 13(6): 603–609.

———, 1992. Satellite remote sensing of forest type and landcover classes in the Subalpine Forest Region, Kananaskis Valley, Alberta, *GeoCarto International*, 7(4): 25–35.

Franklin, S. E., C. F. Blodgett, S. Mah, and C. Wrightson, 1991. Sensitivity of CASI data to anisotropic reflectance, terrain aspect and deciduous forest species, *Canadian Journal of Remote Sensing*, 17(4): 314–321.

Franklin, S. E., and B. A. Wilson, 1992. A three-stage classifier for remote sensing of mountain environments, *Photogrammetric Engineering & Remote Sensing*, 58(4): 449–454.

Gong, P., and P. Howarth, 1990. An assessment of some factors influencing multispectral land-cover classification, *Photogrammetric Engineering & Remote Sensing*, 56(5): 597–603.

Gong, P., R. Pu, and J. R. Miller, 1992. Correlating leaf area index of ponderosa pine with hyperspectral CASI data, *Canadian Journal of Remote Sensing*, 18(4): 275–282.

Gower, J. F. R., and G. A. Borstad, 1990. Mapping of phytoplankton by solar-stimulated fluorescence using an imaging spectrometer, *International Journal of Remote Sensing*, 11: 313–320.

Gower, J. F. R., G. A. Borstad, C. D. Anger, and H. R. Edel, 1992. CCD-based imaging spectroscopy for remote sensing: the FLI and CASI programs, *Canadian Journal of Remote Sensing*, 18(4): 199–208.

Guyot, G. D., D. Guyon, and J. Riom, 1989. Factors affecting the spectral response of forest canopies: a review, *GeoCarto International*, 3: 3–18.

Hall, R., R. Morton, and R. Nesby, 1989. A comparison of existing models for DBH estimation from large-scale photos, *The Forestry Chronicle*, April, pp. 114–120.

Hall-Konyves, K., 1987. The topographic effect on Landsat data in

gently undulating terrain in southern Sweden, *International Journal of Remote Sensing,* 8(2): 157–168.

Hegyi, F., P. Pilon, and P. Walker, 1992. Replacing aerial photos in resource inventories with airborne digital data and GIS, *Proceedings, ASPRS/ACSM/RT 92 Technical Papers,* Washington, D.C., 5: 510–516.

Holben, B. N., and C. O. Justice. 1981. An examination of spectral band ratioing to reduce the topographic effect on remotely sensed data, *International Journal of Remote Sensing,* 2(2): 115–133.

Hopkins, P. F., A. Maclean, and T. Lillesand, 1988. Assessment of Thematic Mapper imagery for forest applications under Lake States conditions, *Photogrammetric Engineering & Remote Sensing,* 54(1): 61–68.

Horler, D. N. H., and F. J. Ahern, 1986. Forestry information content of Thematic Mapper data, *International Journal of Remote Sensing.* 7(3): 405–428.

Hughes, J. S., D. L. Evans, and P. Y. Burns, 1986. Identification of two southern pine species in high resolution aerial MSS data, *Photogrammetric Engineering & Remote Sensing,* 52(8): 1175–1180.

Hutchinson, C. F., R. A. Schowengerdt, and L. R. Baker, 1990. A two-channel multiplex video remote sensing system, *Photogrammetric Engineering & Remote Sensing,* 56(8): 1125–1128.

Irons, J. R., B. Johnson, and G. Linebaugh, 1987. Multiple-angle observations of reflectance anisotropy from an airborne linear array sensor, *IEEE Transactions on Geoscience and Remote Sensing,* 25(3): 372–383.

Irons, J. R., K. J. Ranson, D. Williams, R. Irish, and F. Huegel, 1991. An off-nadir-pointing imaging spectroradiometer for terrestrial ecosystem studies, *IEEE Transactions on Geoscience and Remote Sensing,* 29(1): 66–74.

Ivanco, T., C. Wrightson, D. Cosandier, and M. Chapman. 1991. Image correction and positioning for the Compact Airborne Spectrographic Imager, *Proceedings, 14th Canadian Symposium on Remote Sensing,* Calgary, Alberta, p. 463 (abs.).

Jupp, D. L., A. H. Strahler, and C. E. Woodcock, 1988. Autocorrelation and regularization in digital images I. Basic theory, *IEEE Transactions on Geoscience and Remote Sensing,* 26(4): 463–473.

———, 1989. Autocorrelation and regularization in digital images II. Simple image models, *IEEE Transactions on Geoscience and Remote Sensing,* 27(3): 247–258.

Khorram, S., J. A. Brockhaus, R. I. Bruck, and M. V. Campbell, 1990. Modeling and multitemporal evaluation of forest decline with Landsat TM ditigal data, *IEEE Transactions on Geoscience and Remote Sensing,* 28(4): 746–748.

Kirby, C. L., 1973. *The Kananaskis Forest Experimental Station, Alberta,* Canadian Forest Service Northern Forest Research Centre Information Report, NOR-X-51, Edmonton, Alberta, 50p.

Kriebel, K. T., 1978. Measured spectral bidirectional reflection properties of four vegetated surfaces, *Applied Optics,* 17(2): 249–253.

Leprieur, C. E., J. M. Durand, and J. L. Peyron, 1988. Influence of topography on forest reflectance using Landsat Thematic Mapper and digital terrain data, *Photogrammetric Engineering & Remote Sensing,* 54(4): 491–496.

Miller, J. R., J. Wu, M. G. Boyer, M. Belanger, and E. W. Hare 1991. Seasonal patterns in leaf reflectance red-edge characteristics, *International Journal of Remote Sensing,* 12(7): 1509–1523.

Nakashima, B., G. A. Borstad, D. A. Hill, and R. C. Kerr, 1989. Remote sensing of fish schools, *Proceedings, International Geoscience and Remote Sensing Symposium,* Vancouver, B. C., 2044–2047.

Neville, R. and S. Till, 1991. MEIS-FM, a multispectral imager for forestry and mapping, *IEEE Transactions on Geoscience and Remote Sensing,* 29(1): 184–186.

PCI Inc, 1992. *EASI/PACE Image Analysis System Manuals: Version 5.0,* Toronto, Ontario, variously paged.

Peddle, D. R., and S. E. Franklin, 1991. Image texture processing and data integration for surface pattern discrimination, *Photogrammetric Engineering & Remote Sensing,* 57(4): 413–420.

———, 1992. Multisource evidential classification of land cover and frozen ground, *International Journal of Remote Sensing,* 13(17): 3375–3380.

Peterson, D. L., J. Aber, P. Matson, D. Card, N. Swanberg, C. Wessman, and M. Spanner, 1988. Remote sensing of forest canopy and leaf biochemical contents, *Remote Sensing of Environment,* 24: 85–108.

Plummer, S. E., 1988. Exploring the relationships between leaf nitrogen content, biomass and the Near-Infrared/Red reflectance ratio, *International Journal of Remote Sensing,* 9(1): 177–183.

Ripple, W. J., S. Wang, D. L. Isaacson, and D. P. Paine, 1991. A preliminary comparison of Landsat Thematic Mapper and SPOT-1 HRV multispectral data for estimating coniferous forest volume, *International Journal of Remote Sensing,* 12: 1971–1977.

Royer, A., N. T. O'Neill, D. Williams, P. Cliche, and R. Verreault, 1989. Systeme de mesures de reflectances pour les spectrometres imageurs, *Proceedings, International Geoscience and Remote Sensing Symposium,* Vancouver, Canada, pp. 2097–2099.

Running, S., R. Nemani, D. Peterson, L. Band, D. Potts, L. Pierce, and M. Spanner, 1989. Mapping regional forest evapotranspiration and photosynthesis by coupling satellite data with ecosystem simulation, *Ecology,* 70(4): 1090–1101.

Skidmore, A. K., and B. J. Turner, 1988. Forest mapping accuracies are improved using a supervised nonparametric classifier with SPOT data, *Photogrammetric Engineering & Remote Sensing,* 54(10): 1415–1421.

Spann, M., and R. Wilson, 1985. A quadtree approach to image segmentation which combines statistical and spatial information, *Pattern Recognition,* 18(3/4): 257–269.

SPSSx Inc., 1986. *SPSSx User's Guide,* Second Edition, Chicago, Ill., 988p.

Staenz, K., 1992. A decade of imaging spectrometry in Canada, *Canadian Journal of Remote Sensing,* 18(4): 187–197.

Strahler, A. H., C. E. Woodcock, and J. A. Smith, 1986. On the nature of models in remote sensing, *Remote Sensing of Environment,* 20: 121–139.

Thomas, I. L., 1980. Spatial postprocessing of spectrally classified Landsat data, *Photogrammetric Engineering & Remote Sensing,* 49(9): 1201–1206.

Vlcek, J., and D. King, 1985. Development and use of a 4-camera video system, *Proceedings, 19th International Symposium on Remote Sensing of Environment,* ERIM, Ann Arbor, Michigan, pp. 483–489.

Vogelman, J. E., and B. N. Rock, 1986. Assessing forest decline in coniferous forests of Vermont using NS-001 Thematic Mapper Simulator data, *International Journal of Remote Sensing,* 7(10): 1303–1321.

Walsh, S. J., 1987. Variability of Landsat MSS spectral response of forests in relation to stand and site characteristics, *International Journal of Remote Sensing,* 8(9): 1289–1299.

Williams, D. L., and R. F. Nelson, 1986. Use of remotely sensed data for assessing forest stand conditions in the eastern United States, *IEEE Transactions on Geoscience and Remote Sensing,* 24(1): 130–138.

Woodcock, C. 1982, *Reducing the Influence of Topography on the Classification of Remotely Sensed Data,* Unpubl. M.A. Thesis, UC-Santa Barbara, 69p.

Yuan, X., D. King, and J. Vlcek, 1991. Sugar maple decline assessment based on spectral and textural analysis of multispectral aerial videography. *Remote Sensing of Environment,* 37:47–54.

Zacharias, M., O. Niemann, and G. A. Borstad, 1992. An assessment and classification of a multispectral bandset for the remote sens-

ing of intertidal seaweeds, *Canadian Journal of Remote Sensing*, 18(4): 263–274.

(Received 11 October 1991; revised and accepted 3 March 1993).

Steven E. Franklin
Steven E. Franklin obtained the BES, MA, and PhD (Geography) degrees from the Faculty of Environmental Studies at the University of Waterloo after studies in the School of Forestry at Lakehead University and the Geophysical Institute of the University of Bergen. He held an NSERC Postdoctoral Fellowship and taught remote sensing for two years at Memorial University. In 1988 he moved to the University of Calgary where he is an associate professor in the Department of Geography. Presently he is an Associate Editor of the *Canadian Journal of Remote Sensing* and a Regional Chairman of the Canadian Remote Sensing Society.

glint - Angular variations in the direction from which radio waves arrive at an antenna, and caused by interference at the object.

Global Positioning System (GPS) - The NAVigation Satellite Timing and Ranging (NAVSTAR) GPS is a passive, satellite-based, navigation system operated and maintained by the Department of Defense (DoD). Its primary mission is to provide passive global positioning/navigation for land-, air- and sea-based strategic and tactical forces. A GPS receiver is simply a range measurement device: distances are measured between the receiver point and the satellites, and the position is determined from the intersections of the range vectors. These distances are determined by a GPS receiver which accurately measures the time it takes a signal to travel from the satellite to the station. This measurement process is similar to that used in conventional pulsing marine navigation systems and in phase comparison electronic distance measurement land surveying equipment.

globe - (1) A spherical body. (2) The Earth or the surface of the Earth. (3) A sphere on which a map is shown. In astronomy and geodesy, globe usually denotes a sphere on which is a map of the Earth (terrestrial globe) or of the heavens (celestial globe). SEE ALSO horizon ring; meridian ring; time dial.

globe, celestial - A sphere on which the locations and brightness of stars and other celestial bodies are shown by symbols. The outlines or boundaries of constellations usually are shown also. The celestrial globe commonly has a blue background on which stars are indicated by black or white dots whose sizes are proportional to the stellar magnitudes. Great circles on the globe indicate meridians of right ascension; small circles parallel to the equatorial circle indicate